ARTICLE OPEN

Check for updates

Using multimodal cortical parcellations to identify novel regions of the human cerebral cortex associated with cognitive performance

Shizheng Qiu[1], Zhishuai Zhang[1], Haozheng Liang[1], Jirui Guo[1], Huanyu You[1], Yang Hu[1]✉, Jingjing Liu[2]✉ and Yadong Wang[1,3,4]✉

Cognitive performance has been found to be associated with the complex structure of human cerebral cortex. However, due to the limitations of previous cortical parcellation atlases, the cortical genetic patterns determining cognitive performance remain unknown. Here, we utilized the latest Human Connectome Project Multi-Modal Parcellation (HCP-MMP) atlas to divide the cerebral cortex into 180 regions per hemisphere. We investigated the shared genetic architecture between four types of magnetic resonance imaging (MRI)-derived cortical phenotypes and cognitive performance using large-scale genome-wide association studies (*N* for cortical phenotypes = 36,843; *N* for cognitive performance = 257,828). We observed extensive genetic overlap between cortical surface area, volume, and local gyrification index (LGI) with cognitive performance, particularly the subregions in the insula, cingulate cortex, and ventromedial prefrontal cortex, many of which were novel findings. However, the thickness of some prefrontal regions was negatively correlated with cognitive performance. We identified 18 and 312 shared genetic loci for global and regional cortical phenotypes with cognitive performance, respectively. These genetic loci were involved in a substantial number of biological processes related to neuronal development, cell growth, and neuronal death or apoptosis. The cortical patterns defined by these shared loci were established entirely along the sensorimotor-association (S-A) axis. These findings provide new insights into the genetic relationship between cognitive performance and the human cerebral cortex under a more refined multimodal cortical parcellation scheme.

Translational Psychiatry (2026)16:24 ; https://doi.org/10.1038/s41398-025-03803-8

INTRODUCTION

The cerebral cortex is the outermost layer of the brain, displaying intricate convex (gyral) and concave (sulcal) [1]. These complex cortical structures form the foundation of cognitive performance [2]. Previous studies have revealed that transmodal association cortices, such as the prefrontal cortex and parietal lobe, are responsible for higher-order cognitive functions in humans and have undergone significant expansion over millions of years [3, 4]. However, due to the lack of fine-grained parcellation of higher-order cognitive regions in previous Brodmann areas (52 areas per hemisphere) and Desikan-Killiany atlases (34 areas per hemisphere), as well as the absence of consideration for multi-modal neuroimaging features, the correlations between regional cortical structure and cognitive abilities remain unknown [2, 5–13].

Due to neuroplasticity, cognitive and memory training may reorganize neural circuits in the brain, forming new communication pathways between neurons, thereby leading to changes in brain structure [14–16]. For example, arithmetic training in children may result in changes in cortical thickness in the right temporal lobe and left occipital gyrus, while memory training in older adults may lead to changes in the thickness of the right fusiform and lateral orbitofrontal cortex [17, 18]. Hence, it remains unclear whether cognitive performance is the cause or the consequence of changes in brain structure.

Previous genetic studies have examined the relationships between cortical structure and cognitive performance using genome-wide association studies (GWAS). For instance, Jansen et al. revealed genomic loci shared between brain volume and intelligence [12]. However, these studies also relied on coarser parcellation schemes, which limited the spatial resolution for identifying region-specific genetic associations, particularly in association cortices that have undergone significant evolutionary expansion and are critical for higher-order cognitive functions.

In this study, we parcellated the cerebral cortex into 180 regions per hemisphere using the Human Connectome Project Multi-Modal Parcellation (HCP-MMP) atlas, which took into account the anatomical, functional, and connectivity characteristics of the cortex. We investigated the genetic correlations and bidirectional causal relationships between cognitive performance and magnetic resonance imaging (MRI)-derived cortical measures (cortical surface area, thickness, volume, and local gyrification index (LGI)) using large-scale GWAS summary statistics ($N > 250{,}000$) [19–22]. We employed conjunctional false discovery rate (conjFDR) to identify shared lead-single-nucleotide polymorphisms (SNPs)

[1]Faculty of Computing, Harbin Institute of Technology, Harbin, China. [2]Eye Hospital, the First Affiliated Hospital of Harbin Medical University, Harbin, China. [3]School of Medicine and Health, Harbin Institute of Technology, Harbin, China. [4]Zhengzhou Research Institute, Harbin Institute of Technology, Zhengzhou, China. ✉email: huyang@hit.edu.cn; liujingjing4700@126.com; ydwang@hit.edu.cn

Received: 1 July 2025 Revised: 19 November 2025 Accepted: 15 December 2025
Published online: 12 January 2026

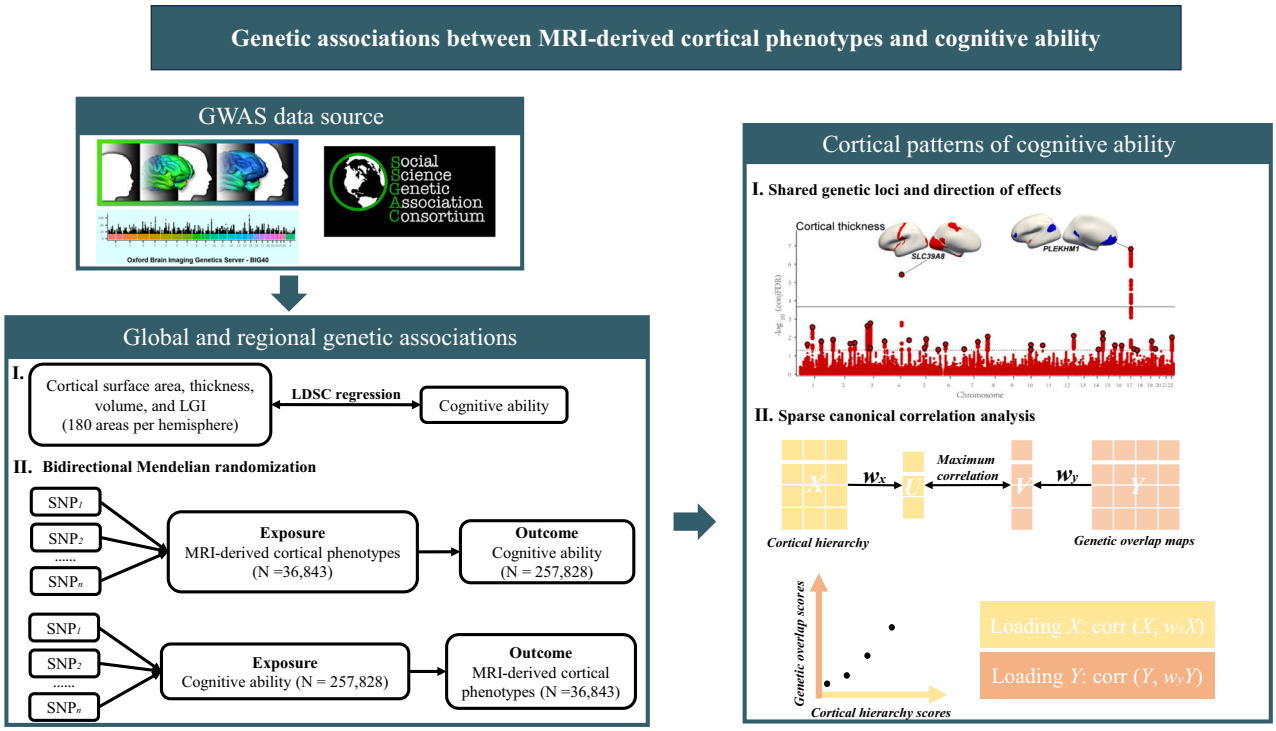

Fig. 1 Study design.

associated with both cortical structures and cognitive performance [23, 24]. Based on these shared loci, we assessed whether the cortical patterns determining cognitive performance align with the anatomical, functional, and evolutionary hierarchies of the sensorimotor-association (S-A) cortical axis. Finally, we mapped these SNPs to genes within brain tissues and elucidate the shared genetic basis and underlying biological mechanisms between cerebral cortex and cognitive performance (Fig. 1).

RESULTS

Genetic correlations at 180 cortex regions

According to the HCP-MMP atlas, we parcellated the human cerebral cortex into 180 regions per hemisphere, with detailed descriptions of each region provided in Fig. 2 **and** Supplementary Table 1 [25]. We first investigated the genetic correlations between global and 180 regional cortical phenotypes and cognitive performance using linkage disequilibrium score regression (LDSR). Global cortical surface area (rg = 0.222, $P = 2.69E-15$), volume (rg = 0.235, $P = 1.27E-15$), and LGI (rg = 0.098, $P = 1.70E-03$) were positively correlated with cognitive performance (Supplementary Table 2). However, global cortical thickness did not show significant association with cognitive performance (rg = 0.0098, $P = 0.73$). As illustrated in the genetic overlap map in Fig. 3A, cortical surface area and volume exhibited positive correlations with cognitive performance across all cortical regions. However, cortical thickness in parts of the anterior cingulate cortex, dorsolateral prefrontal cortex, and anterior prefrontal cortex, which were associated with higher-order brain functions, showed negative correlations with cognitive performance ($P < 0.05$). Cortical LGI in portions of the superior parietal lobule, which was involved in spatial orientation and working memory functions in the brain, exhibited negative correlations with cognitive performance. After multiple testing ($P < 0.05/180 = 0.000278$), cognitive performance exhibited a significant positive correlation with cortical surface area across 161 regions, cortical volume across 134 regions, cortical LGI across 34 regions, and cortical, thickness across 2 regions (Supplementary Table 3).

Bidirectional causal relationships

We conducted bidirectional Mendelian randomization (MR) analyses to assess the directionality of the causal relationship between genetically proxied cortical measurements and cognitive performance. We found that global cortical surface area, LGI, and volume exhibited bidirectional causal relationships with cognitive performance. Specifically, greater cortical surface area ($\beta = 0.144$, 95%CI: 0.106–0.183, $P = 2.17E-13$), volume ($\beta = 0.181$, 95%CI: 0.139–0.222, $P = 9.05E-18$), and LGI ($\beta = 0.088$, 95%CI: 0.045–0.131, $P = 5.83E-05$) were associated with higher cognitive performance, while conversely, higher cognitive performance was associated with increased cortical surface area ($\beta = 0.215$, 95%CI: 0.149–0.281, $P = 1.61E-10$), volume ($\beta = 0.233$, 95%CI: 0.171–0.294, $P = 1.75E-13$), and LGI ($\beta = 0.118$, 95%CI: 0.051–0.185, $P = 0.000567$) (Supplementary Table 4-5). However, global cortical thickness was not associated with cognitive performance. These findings aligned with the hypothesis of brain plasticity.

Furthermore, we investigated the causal effects of cortical measurements at 180 specific regions on cognitive performance, vice versa. The cortical surface area and volume of many regions in the insula, sensorimotor cortex, dorsolateral prefrontal cortex, frontal eye fields, cingulate cortex, parahippocampal region, temporal gyrus, and temporoparietooccipital junction area exhibited bidirectional causal relationships with cognitive performance. Specifically, after FDR correction, increased thickness in 2 cortical regions, LGI in 20 cortical regions, surface area in 83 cortical regions, and volume in 60 cortical regions were significantly associated with enhanced cognitive performance. Higher cognitive performance was significantly correlated with greater thickness in 1 cortical region, LGI in 5 regions, surface area in 70 regions, and volume in 75 regions. However, the thickness of area 6 mp, area anterior 47r, ventromedial visual area, presubiculum, posterior inferotemporal complex, area PFcm, area a24, area STSd anterior (anterior superior temporal sulcus dorsal), parts of area 9 (in the dorsolateral prefrontal cortex), and portions of the area 32 (superior anterior cingulate cortex) and the LGI of area 7 A and area PFt were negatively correlated with cognitive performance, even without passing multiple testing corrections

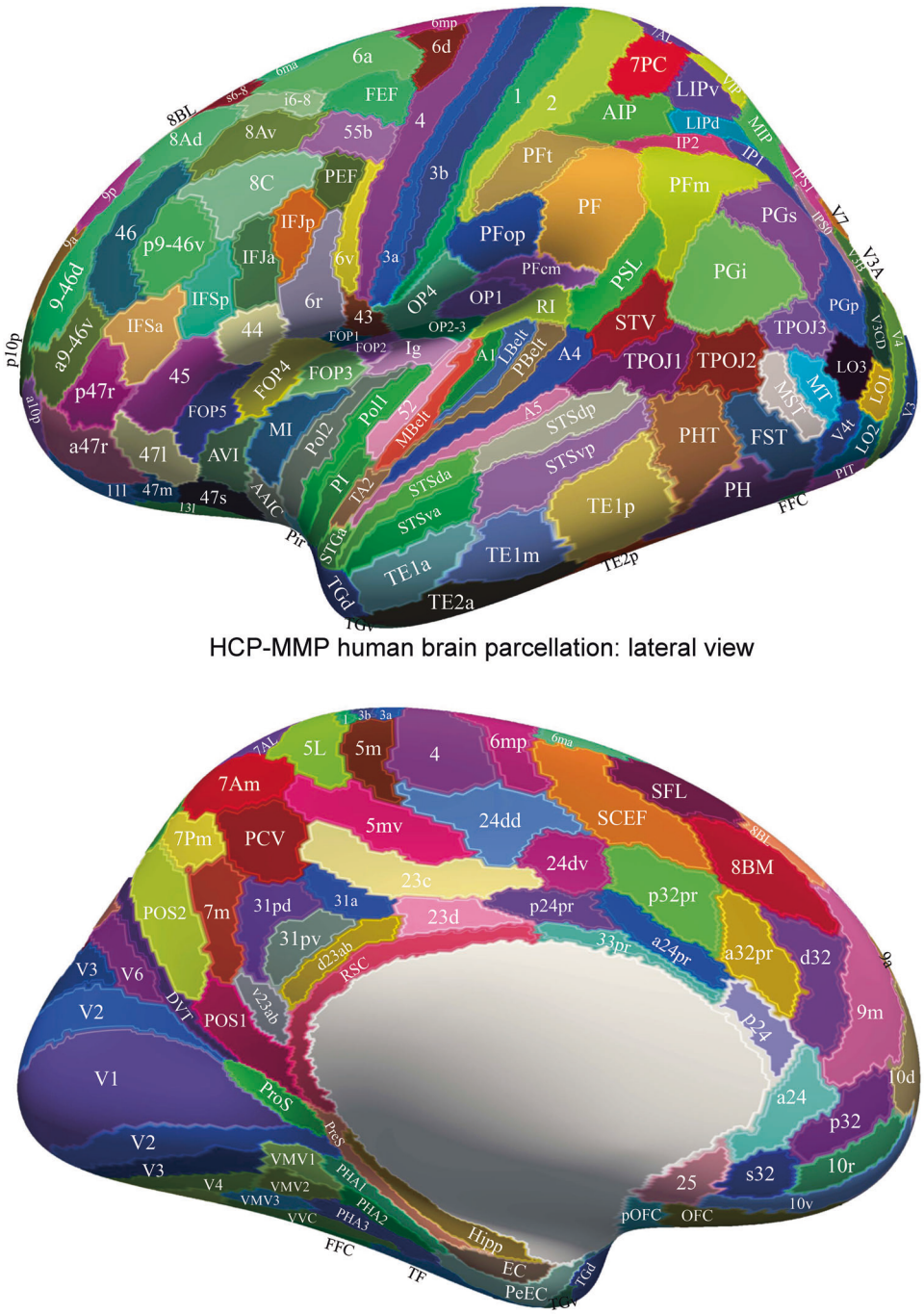

Fig. 2 Human cortical regions in the HCP-MMP atlas. The sulci were expanded sufficiently to allow the regions within the sulci to be shown. The names and descriptions of the 180 regions from the HCP-MMP atlas were provided in Supplementary Table 1.

(0.05/180 < P < 0.05) (Fig. 3B-C, Supplementary Table 6-7). These cortical regions may influence different aspects of cognitive performance. For instance, area 47 is involved in semantic processing, while area PFcm is related to phonological storage [26, 27]. Presubiculum, as part of the hippocampal formation, is associated with memory [28]. Area 9 is implicated in various functions such as short-term memory, inferring the intentions of others, inductive reasoning, and sustained attention [29–32]. Area 32 is responsible for the processes of decision-making and emotional control. It is noteworthy that among all the cortical measurements, the volume of the posterior insular area 1 exhibited the strongest causal effect on cognitive performance ($\beta = 0.198$, 95%CI: 0.138–0.259, $P = 1.67E\text{-}10$), while cognitive performance had the greatest influence on the volume of area 1 (in the somatosensory cortex) ($\beta = 0.261$, 95%CI: 0.174–0.349, $P = 5.67E\text{-}09$). Additionally, MR-Egger results indicated that only a few analyses exhibited potential pleiotropy (Supplementary Table 6-7).

Shared genetic loci between global cortical phenotypes and cognitive performance

Using conditional Quantile-Quantile (Q-Q) plots, we compared the distribution of SNPs associated with cortical phenotypes and

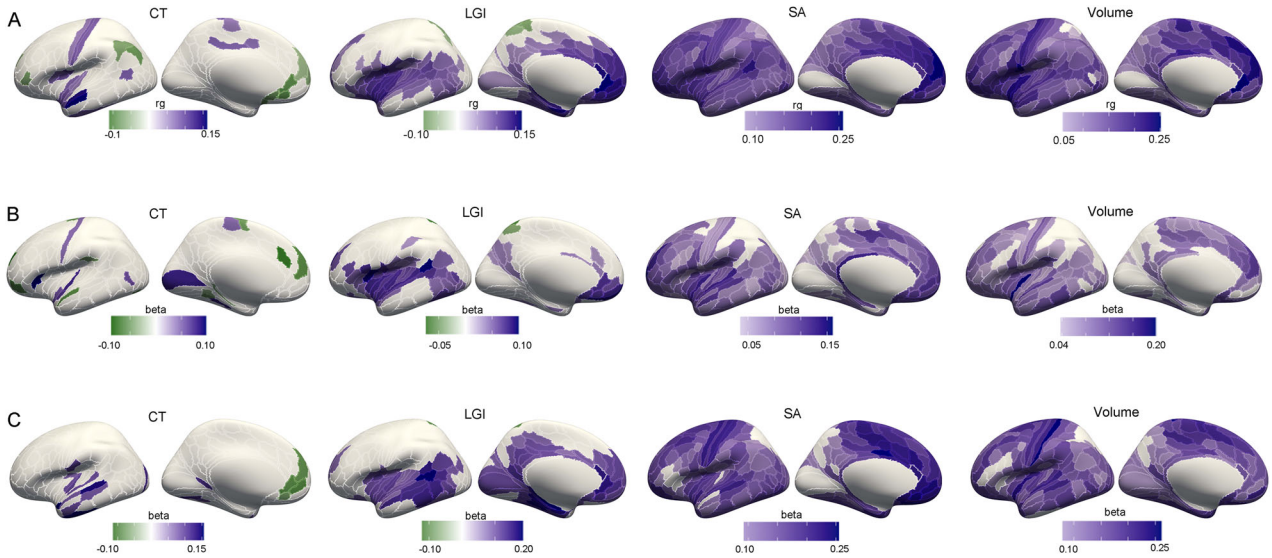

Fig. 3 Genetic associations and casual relationships of regional cortical phenotypes and cognitive performance using LDSC regression and MR analysis. In the maps, blue color indicates a positive association between cortical phenotypes and cognitive abilities in this cortical region, while the green color signifies a negative association between cortical phenotypes and cognitive abilities in this cortical area. Only display the cortical regions with significant associations ($P < 0.05$). Cortical measurements were defined as the average values of the left and right hemispheres, with the left hemisphere being exemplified in the figure. **A** Genetic correlations of regional cortical phenotypes and cognitive performance. **B** Casual effects of regional cortical phenotypes on cognitive performance. **C** Casual effects of cognitive performance on regional cortical phenotypes.

cognitive performance. We observed significant pleiotropic enrichment in all MRI-derived cortical phenotypes related to cognitive performance, as evidenced by points in the Q-Q plot significantly deviating from the 45-degree diagonal line (Supplementary Fig. 1). For each MRI-derived cortical phenotypes and cognitive performance phenotype pair, we identified the shared genetic loci using conjFDR statistical framework. Following rigorous multiple testing corrections (conjFDR < 0.05/180 = 0.000278), we identified 18 shared lead-SNPs for MRI-derived cortical phenotypes and cognitive performance (Table 1, Fig. 4). Specifically, 2 loci were associated with cortical thickness and cognitive performance, 2 with cortical LGI and cognitive performance, 11 with cortical surface area and cognitive performance, and 10 with cortical volume and cognitive performance. Among these loci, rs768023 (*FOXO3*) exhibited the strongest association between cortical phenotypes and cognitive performance (conjFDR = 1E-09). Additionally, rs56192752 (*PLEKHM1*) showed associations with all four cortical phenotypes (conjFDR for cortical surface area = 7.07E-08, conjFDR for cortical thickness = 1.48E-07, conjFDR for cortical volume = 6.84E-08, conjFDR for cortical LGI = 1.39E-07), while rs10876864 (*IKZF4*), rs17698176 (*NSF*), rs2764264 (*FOXO3*), and rs11079849 (*IGF2BP1*), and exhibited associations with two cortical phenotypes and cognitive performance.

Subsequently, we observed the effect directions of these genetic loci across 180 cortical regions. Consistent effect directions of lead-SNPs on both cortical phenotypes and cognitive performance implied that higher cognitive performance was associated with thicker cortical thickness, larger surface area, larger volume, or more complex LGI, while the converse suggested that higher cognitive performance was linked to thinner cortical thickness, smaller surface area, smaller volume, or simpler LGI. The majority of genetic loci exhibited concordant direction of effects in all regions (Supplementary Table 8). However, rs56192752 (*PLEKHM1*) demonstrated a consistent direction of effect on cognitive performance and cortical thickness of area TA2 (in the auditory association cortex), indicating that thicker cortical thickness in the area TA2 were associated with higher cognitive performance, and an inconsistent direction of effect on cognitive performance and cortical thickness of other regions, suggesting that thicker cortical thickness in these regions were associated with lower cognitive performance (Fig. 4A).

Regional cortical patterns of cognitive performance

After FDR correction (conjFDR < 0.05/180 = 0.000278), we identified 45, 59, 178, and 163 independent lead-SNPs shared with regional cortical thickness, LGI, surface area, and volume and cognitive performance, respectively (Fig. 5A, Supplementary Table 9). We observed the highest genetic overlap in the cortical volume of the posterior insular area 2 and cognitive performance, with 11 shared genetic loci. As depicted in Fig. 5A, the genetic overlap distribution of cognitive performance with cortical surface area and volume was similar, with a higher number of overlapping genetic loci observed in the sensorimotor cortex, insular cortex, part of cingulate cortex, primary visual cortex, and auditory cortex. Although there were fewer shared genetic loci between cognitive performance and cortical thickness or LGI, overlaps were still observed in the primary visual cortex, part of cingulate cortex, part of insular cortex, perirhinal ectorhinal cortex, parieto-occipital sulcus area 1, and dorsolateral prefrontal cortex.

The spatiotemporal patterning of cortical maturation proceeded in a hierarchical manner, conforming to an evolutionarily rooted sensorimotor-to-association axis of cortical organization, referred to as the S-A cortical axis [33–36]. Whether the cortical pattern determining cognitive performance aligned with the established anatomical, functional, and evolutionary hierarchies of the S-A cortical axis remained unknown. We defined the number of shared genetic loci between cognitive performance and cortical phenotypes across the 180 regions as the cortical pattern of cognitive performance. We employed sparse canonical correlation analysis (sCCA) to identify multivariate associations between the cortical pattern of cognitive performance and the S-A cortical axis. We observed a moderate correlation ($r = 0.344$, $P < 0.001$), accounting for 11.82% of the covariance. The cortical pattern of cognitive performance had the highest positive canonical loading on the functional hierarchy (G1.fMRI = 0.998) (Supplementary Table 10). The anatomical hierarchy (T1w/T2w = −0.578, neuroanatomical gradient negatively correlated with the anatomical

Table 1. Shared genetic loci of global cortical phenotypes and cognitive performance using conjFDR.

Cortical phenotype	SNP	Nearest Gene	A1	A2	CHR	Position	conjFDR	P_{cortex}	$P_{cognition}$
Thickness	rs13107325	*SLC39A8*	C	T	4	103188709	3.71E-06	8.26E-09	2.72E-19
Thickness	rs56192752	*PLEKHM1*	A	G	17	43555253	1.48E-07	1.22E-10	3.12E-10
LGI	rs7663887	*LCORL*	C	A	4	17902920	0.000113	5.46E-07	9.78E-08
LGI	rs56192752	*PLEKHM1*	A	G	17	43555253	1.39E-07	2.35E-16	3.12E-10
Surface area	rs9813691	*STAG1*	T	G	3	136260722	8.97E-05	8.14E-07	9.68E-07
Surface area	rs1391438	*TET2*	T	C	4	106151843	0.000165	1.63E-06	7.56E-07
Surface area	rs6820810	*LCORL*	G	A	4	17866325	3.67E-06	2.47E-08	1.92E-08
Surface area	rs2362109	*MEF2C*	C	T	5	88148041	0.00007	6.13E-07	1.29E-07
Surface area	rs2764264	*FOXO3*	C	T	6	108934461	4.8E-08	2.56E-10	3.21E-12
Surface area	rs41563	*SRPK2*	G	A	7	104852654	0.000193	1.46E-06	2.53E-06
Surface area	rs10876864	*IKZF4*	G	A	12	56401085	2.22E-05	2.18E-15	1.92E-07
Surface area	rs965770	*C14orf177*	C	T	14	98583045	0.000136	1.07E-06	1.66E-06
Surface area	rs11079849	*IGF2BP1*	C	T	17	47090785	2.97E-06	1.97E-08	4.7E-09
Surface area	rs17698176	*NSF*	T	G	17	44819595	4.54E-05	2.74E-11	4.45E-07
Surface area	rs56192752	*PLEKHM1*	A	G	17	43555253	7.07E-08	3.4E-37	3.12E-10
Volume	rs13064576	*BSN*	C	T	3	49642430	3.02E-05	2.19E-07	1.72E-17
Volume	rs67214626	*PCCB*	C	T	3	135989376	9.01E-05	1.68E-08	1.09E-06
Volume	rs1909122	*TET2*	C	T	4	106127004	0.000254	6.89E-07	3.68E-06
Volume	rs7671110	*LCORL*	C	T	4	17874089	2.34E-05	1.66E-07	6.29E-08
Volume	rs2764264	*FOXO3*	C	T	6	108934461	1E-09	2.89E-13	3.21E-12
Volume	rs10876864	*IKZF4*	G	A	12	56401085	2.07E-05	1.15E-10	1.92E-07
Volume	rs2293446	*PRKAG1*	G	A	12	49412709	1.19E-05	8.02E-08	6.17E-12
Volume	rs11079849	*IGF2BP1*	C	T	17	47090785	4.79E-06	3.02E-08	4.7E-09
Volume	rs17698176	*NSF*	T	G	17	44819595	4.24E-05	8.2E-10	4.45E-07
Volume	rs56192752	*PLEKHM1*	A	G	17	43555253	6.84E-08	4.45E-17	3.12E-10

LGI local gyrification index.

hierarchy) and evolutionary hierarchy (Evolution.Expansion = 0.326) also showed positive correlations with the cortical pattern of cognitive performance.

We further assessed the consistency of the direction of effect for these shared genetic loci in regional cortical phenotypes and cognitive performance. Homogeneity in the direction of effect for shared genetic loci would support a common genetic basis between cortical structure and cognitive performance, while heterogeneity, particularly in the direction of effect of SNPs influencing the same cortical region, would support distinct biological mechanisms [37]. We observed nearly complete consistency or inconsistency in the direction of effect for cortical phenotypes and cognitive performance in the same cortical regions (blue or green), suggesting a shared genetic basis for cortical phenotypes and cognitive performance in most regions, where these loci might influence cognitive performance through regional cortical phenotypes (Fig. 5B, Supplementary Table 9). However, some shared genetic loci exhibited mixed directions of effect sizes on cortical measurements (e.g., cortical surface area in many regions near the temporal gyrus, LGI in the primary motor cortex) and cognitive performance for the same region, suggesting distinct genetic underpinnings for these regions.

Functional annotation

Due to the majority of shared SNPs being located in non-coding regions, we conducted functional annotation (Supplementary Fig. 2). The shared SNPs were classified using the RegulomeDB variant classification scheme. One shared SNP (rs6445538) for cortical thickness and cognitive performance, two SNPs (rs7638808 and rs10876864) for cortical LGI and cognitive performance, and three SNPs (rs4753000, rs10876864, and rs10499) for cortical surface area and cognitive performance were classified as category 1, indicating that they might affect transcription factor binding and be linked to the expression of gene targets (Supplementary Table 11) [38]. All these SNPs were located in open chromatin states regions; these SNPs annotated to *TMEM110*, *SMIM4*, *IKZF4*, *PSMC3*, and *ATP2A1* as nearest genes, respectively. We utilized the Braineac eQTL dataset to investigate the gene regulatory effects of these 5 SNPs (Supplementary Table 12). Only rs6445538 C allele was significantly associated with upregulated expression of *ITIH4* across 8 brain tissues (cerebellar cortex, frontal cortex, hippocampus, inferior olivary nucleus, putamen, temporal cortex, thalamus, and intralobular white matter) and passed multiple testing (Supplementary Fig. 3). The *NEK4-ITIH1-ITIH3-ITIH4* region has been implicated in mood disorders, anxiety-like behaviors, and social behavior deficits, with *ITIH1* and *ITIH3* exhibiting stronger effects compared to *ITIH4* [39]. We further replicated these findings using the eQTL dataset from the Genotype-Tissue Expression (GTEx) project. The rs6445538 variant regulated the expression of *ITIH4*, *RFT1*, *SFMBT1*, *PPM1M*, *GNL3* across all 13 brain regions (Supplementary Table 12). The rs7638808 variant regulated the expression of *GNL3*, *SEMA3G*, *NEK4*, *PPM1M*, *GLYCTK*, *ITIH4*, *GLT8D1*, and *POC1A* in cerebellar hemisphere, cerebellum, cortex, hypothalamus, nucleus accumbens basal ganglia, and putamen basal ganglia. The rs10876864 variant regulated the expression of *SUOX* and *RPS26* across all 13 brain regions. The rs4753000 variant regulated the expression of *MTCH2*, *PSMC3*, *MADD*, *ACP2*, and *RAPSN* across 6 brain tissues. The rs10499 variant regulated the expression of 10 genes across all 13 brain regions.

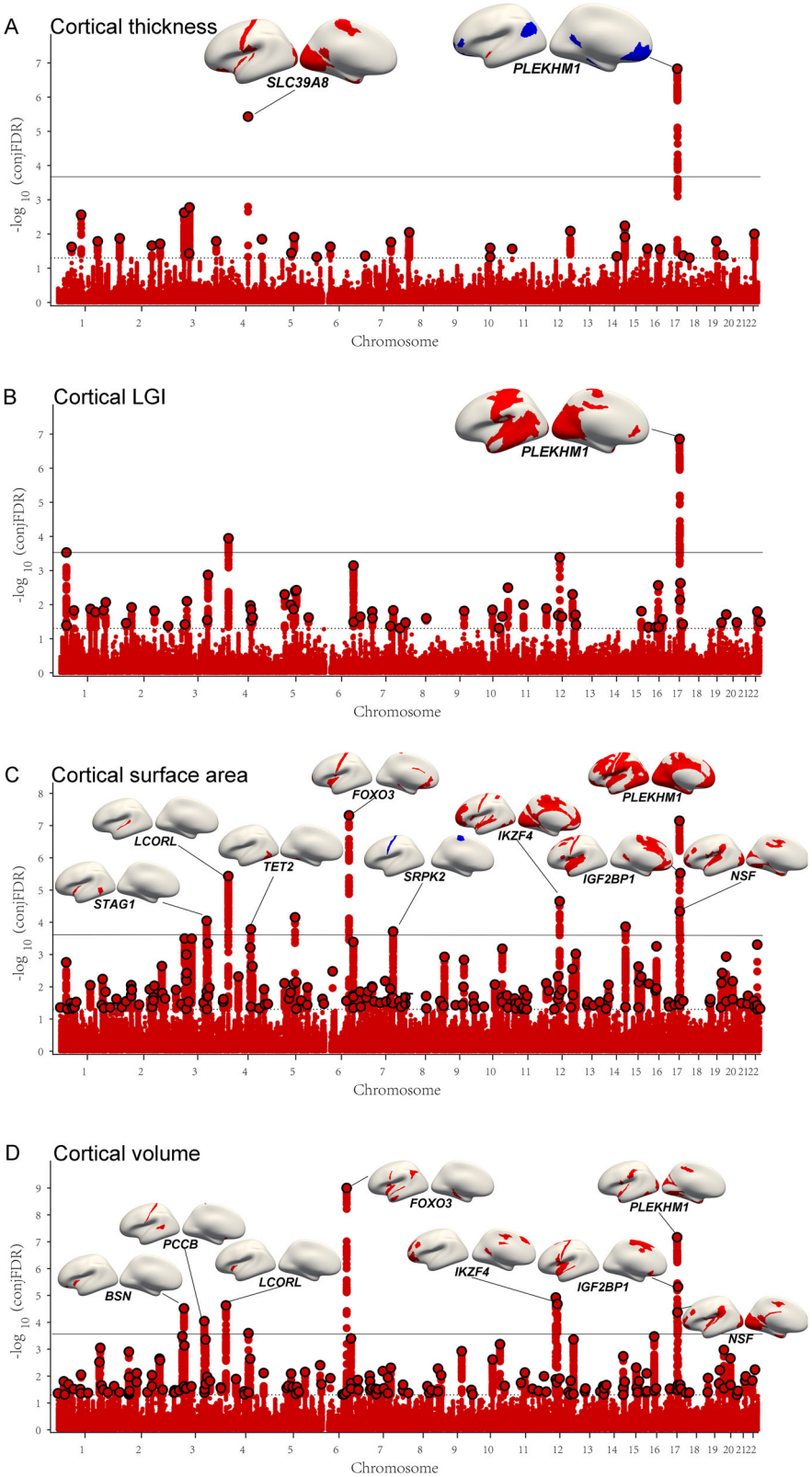

Fig. 4 Manhattan plots of shared genetic loci associated with global cortical phenotypes and cognitive performance at conjFDR < 0.05/180 = 0.000278. A Cortical thickness. **B** Cortical LGI. **C** Cortical surface area. **D** Cortical volume. A black circle around the enlarged data points indicates the lead-SNPs in each LD block. The cortical map illustrates the brain regions that are shared by the lead-SNP with cognitive performance. Red indicates concordant directions of effect, where higher cognitive performance is associated with larger cortical surface area, thicker cortical thickness, larger cortical volume, or more complex LGI. Conversely, blue represents discordant directions of effect, where higher cognitive performance is associated with smaller surface area, thinner thickness, smaller volume, or simpler LGI.

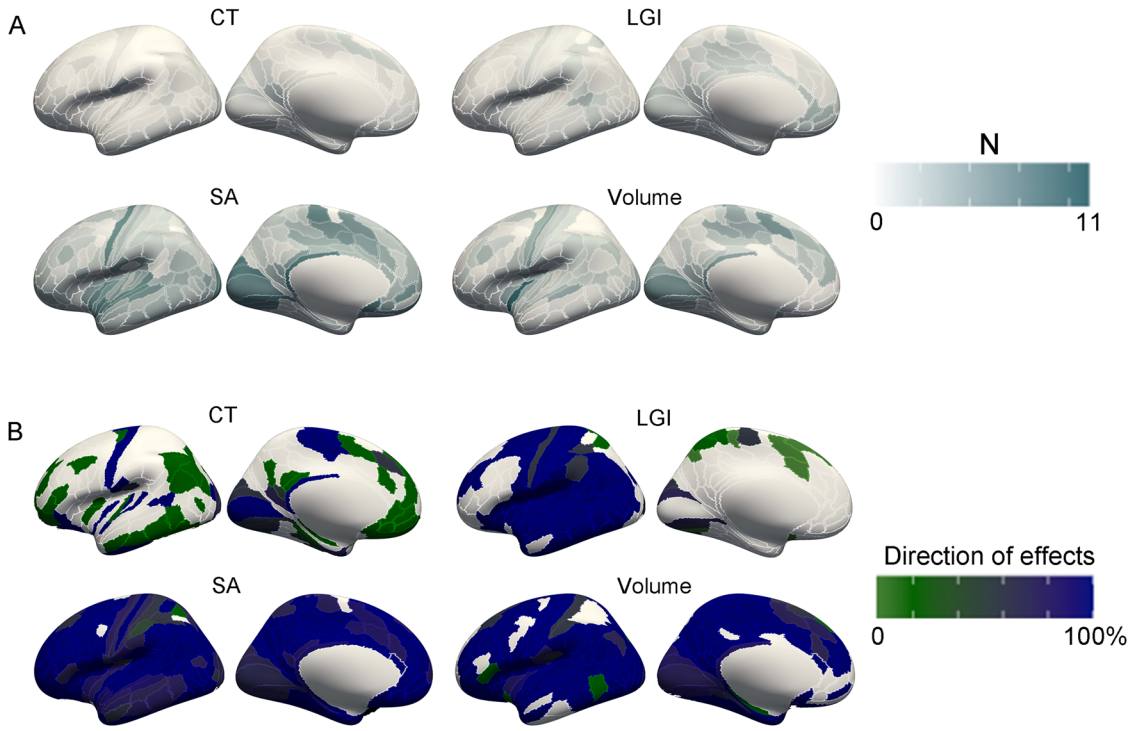

Fig. 5 Shared genetic loci between regional cortical phenotypes and cognitive performance. A The number of shared genetic loci between regional cortical phenotypes and cognitive performance. **B** The effect direction of shared genetic loci between regional cortical phenotypes and cognitive performance. The cortical maps illustrate the percentage of genetic sharing loci exhibiting a consistent effect direction among all loci between regional cortical phenotypes and cognitive performance. In the maps, blue indicates that the number of genetic sharing loci with a consistent effect direction account for 100% of the total number of loci, while green represents that the number of genetic sharing loci with a consistent effect direction account for 0% of the total number of loci.

Enrichment analysis revealed that the genetic loci shared between cortical thickness and cognitive performance are involved in cellular components related to neurons and synapses (Supplementary Fig. 4A, Supplementary Table 13). The genetic loci shared between cortical LGI and cognitive performance participate in biological processes regulating neuronal development and cell growth, as well as cellular components associated with neurons, synapses, and lysosomes (Supplementary Fig. 4B, Supplementary Table 14). The genetic loci shared between cortical surface area and cognitive performance are involved in a wide range of biological processes related to neuronal death or apoptosis (Supplementary Fig. 4C, Supplementary Table 15). The genetic loci shared between cortical volume and cognitive performance participate in the regulation of biological processes related to developmental cell growth, neuron projection development, and neuronal death (Supplementary Fig. 4D, Supplementary Table 16).

DISCUSSION

The complex gyral and sulcal structure of the human cerebral cortex forms the foundation for cognition. However, some cortical regions associated with higher-order cognition have not been precisely delineated. In the current study, we leveraged the HCP-MMP atlas to reveal the genetic relationships between cognitive performance and cortical phenotypes in specific regions. We discovered that cortical surface area, volume, and LGI exhibited similar genetic patterns in certain regions, with cortical thickness being the only divergent cortical measurement. We identified numerous novel regions associated with cognitive performance that have not been previously reported, particularly in the insula and prefrontal cortex, which are implicated in higher-order cognition.

To investigate which cortical phenotypes were significantly correlated with cognitive performance in different regions, we performed bivariate LDSR and MR analyses simultaneously. Cortical surface area exhibited the strongest associations with cognitive performance, with 161 regions showing significant correlations after multiple testing. Among the 180 cortical regions, only the prostriata area and primary visual cortex showed no relationship between their surface area and cognitive performance, both of which are primarily involved in visual processing [40]. These findings suggested that cortical phenotypes (except for cortical thickness) exerted widespread effects on cognition across numerous regions. Interestingly, cortical thickness of certain regions exhibited a negative correlation with cognitive performance (although non-significant after FDR correction), particularly evident in the dorsolateral prefrontal cortex, and anterior prefrontal cortex. An analysis of T1-weighted structural MRI data from over 10,000 samples of children aged 9 to 11 years revealed a higher intelligence quotient correlated with greater cortical thickness in the orbitofrontal cortex but lower cortical thickness in the dorsolateral and ventromedial prefrontal cortex [41]. We speculated that pre-adolescence represented a crucial transitional period where, due to the dynamic nature of neural development, the direction of the correlation between the thickness of certain prefrontal cortical layers and cognitive performance and intelligence might undergo a significant shift before adolescence [41, 42].

MR analyses further supported the extensive causal relationships between the cortical surface area, volume, and cognitive performance in multiple regions. A large number of regions in the prefrontal cortex, insula, hippocampal regions, temporal gyri, and sensorimotor cortices exhibited bidirectional causal associations between their surface area, volume, and cognitive performance. This bidirectional causality aligned with the concept of brain

plasticity, whereby cognitive training and experience could induce structural changes in the brain. However, the thickness of some cortical regions previously reported to be associated with cognition showed negative correlations with cognitive performance, such as presubiculum in the parahippocampal cortex and area 9 anterior in the dorsolateral prefrontal cortex.

In comparison to other mammals positioned lower on the evolutionary tree, humans exhibited a pronounced expansion of the new association cortices, which served advanced functions such as cognition [33, 43, 44]. We conducted sCCA between the distribution pattern of the genetic overlap of regional cortical structure and cognitive performance across 180 cortical regions and the ranking of three cortical hierarchies within the S-A cortical axis across the same 180 cortical regions. Here, we defined the genetic patterns between cortical anatomical features and cognitive performance as the number of shared genetic loci identified by conjFDR. The genetic overlap pattern between cortical structure and cognitive performance might be associated with anatomical, functional, and evolutionary hierarchies within the S-A cortical axis, indicating that the genetic architecture of cognitive performance follows the same spatiotemporal patterning as cortical maturation and evolution, with stronger associations in association cortices. It was worth noting that Mesulam further subdivided the transmodal association zones along the S-A axis into heteromodal association cortices (prefrontal, posterior parietal, lateral temporal, and medial temporal cortices) responsible for cognitive elaboration and control, and paralimbic association cortices (orbitofrontal, ventromedial prefrontal, insular, temporopolar, and cingulate cortices) involved in mentalizing, motivation, and socioemotional processing [33, 45, 46]. A considerable number of regions within both the heteromodal association cortices and paralimbic association cortices were found to be genetically correlated with cognitive performance in present study.

Utilizing the conjFDR statistical framework, we identified 18 and 312 shared genetic loci for cognitive performance with global and regional cortical phenotypes. Some shared genes have already been reported to be associated with cortical structure and/or cognitive performance. *SLC39A8* expression in the brain was associated with the normal development and functional regulation of neurons and was also a risk locus for putamen volume and schizophrenia [47, 48]. *LCORL* regulated the cell cycle and transcription inhibition, serving as a significant locus for brain imaging phenotypes in mild cognitive impairment or Alzheimer's disease [49]. SNP rs11079849 (*IGF2BP1*) was located in the enhancer/promoter region of *IGF2BP1* in the fetal brain, concurrently associated with intracranial volume and general cognitive function [50]. *SH2B1* influenced the neural dendrite formation of cortical neurons [51]. *FOXO3* was renowned for its involvement in longevity and aging regulation, and it was also associated with brain volume and cognitive function [52]. These genes were involved in a substantial number of biological processes related to neuronal development, cell growth, and neuronal death or apoptosis.

Our study has some limitations. In order to facilitate statistical analysis, we defined cortical measurements as the average values of the left and right hemispheres, which may overlook the impact of hemispheric asymmetry on cognitive abilities. Additionally, while global cortical thickness in adults is unrelated to cognitive performance, during prenatal or early childhood stages, cortical thickness may exhibit a positive correlation with cognitive performance [7]. During late childhood or pre-adolescence, there may be a shift in the direction of the correlation between cortical thickness and cognitive performance. Specifically, cortical thickness peaks in the first few years after birth and subsequently declines [53–56]. The cortical structural data utilized in this study are derived from a meta-analysis of the UK Biobank and the Adolescent Brain and Cognitive Development (ABCD) cohorts. Although the genetic correlation between the UK Biobank and ABCD cohort supports the meta-analysis (cortical thickness: $rg = 0.83 \pm 0.04$), participants from the ABCD cohort may be undergoing dynamic neurodevelopmental processes, which could significantly impact the correlation between cortical thickness and cognitive performance [19]. The availability of prenatal or early childhood MRI data would be a valuable supplement to this study. Finally, our investigation solely examines the impact of genetic factors on cortical phenotypes and cognitive performance. The influence of environmental factors remains unclear, and it is imperative for future large-scale longitudinal studies to validate the causal relationships identified in this research.

In conclusion, we provide novel insights into the genetic relationship between cognitive performance and the human cerebral cortex by leveraging a more refined multimodal cortical parcellation scheme.

METHODS

Participants

We accessed GWAS summary statistics for global and regional cortical surface area, thickness, volume, and LGI from a meta-analysis of the UK Biobank and the ABCD study (N = 36,843) by Warrier et al. [19, 57–59]. These neuroimaging measures were estimated across 180 areas per hemisphere bounded by sharp changes in cortical architecture, function, connectivity, and/or topography using the Human Connectome Project Multi-Modal Parcellation (HCP-MMP) atlas [25]. Specifically, the cortical surface was reconstructed for each participant using FreeSurfer (version 7.3.2) and registered using FreeSurfer's surface-based registration to fsaverage. The HCP-MMP was resampled from fs_LR to fsaverage using existing transformations and from there back to the individual's surface meshes based on the FreeSurfer folding-based surface registration [19, 25, 60, 61]. Cortical measurements were averaged for each hemisphere, resulting in 180 bilateral regions. Total cortical surface area was measured at midthickness. Cortical thickness and volume represented average thickness and total volume of the cortex, respectively. LGI was a commonly used measure for quantifying local cortical folding or gyrification, which was calculated by computing the ratio of the surface area between the outer smoothed surface and the inner surface that closely wraps the pial surface [19, 62]. The list of 180 cortical regions of the HCP-MMP atlas was shown in Supplementary Table 1 [25, 60, 63]. The entire preprocessing pipeline is described in detail in Warrier et al. [19].

It is important to note that regional cortical measurements were appropriately adjusted for global brain size measures to isolate region-specific genetic effects. The genetic correlations and shared loci we identified therefore represent the genetic overlap between regional cortical structure (independent of global size) and cognitive performance.

We accessed GWAS summary statistics for cognitive performance (N = 257,828) from a meta-analysis of the UK Biobank and the Cognitive Genomics Consortium (COGENT) by Social Science Genetic Association Consortium (SSGAC) [22]. Participants in the UK Biobank were administered a test of verbal-numerical reasoning, and the mean of standardized scores was computed [22]. For each cohort within the COGENT, participants completed an average of 8 ± 4 neuropsychological tests [22, 64]. Statistics were conducted on the overall accuracy or total number of correct responses across all test variables completed by participants in neuropsychological tests. All samples were of European descent.

Global and regional genetic correlation

Using bivariate LDSR analyses, we assessed the genetic correlations between global and regional cortical phenotypes and cognitive performance [65, 66]. For each SNP, an LD score is computed as the sum of its squared correlations (r^2) with all other SNPs within a specified window. The LD scores were based on the default reference panel of individuals with European ancestry from the 1000 Genome Project. A regression of χ^2 statistics from GWAS summary data on LD scores is performed. The slope of this regression is proportional to the SNP heritability, while the intercept provides an estimate of confounding biases, including population stratification. For pairs of traits, the product of z-scores from two GWAS is regressed on the LD score. The resulting genetic covariance is then normalized by the SNP heritability to obtain the genetic correlation. Significance for genetic associations was defined as $P < 0.05/180 = 0.000278$ after multiple testing.

Mendelian randomization (MR)

The MR model employed the instrumental variable (IV) method to evaluate causal relationships between exposure and outcome factors, relying on three key assumptions: (1) the IVs were significantly associated with exposure, (2) the IVs were not associated with any potential confounder, and (3) the IVs influenced the outcome solely through the exposure and not through any other pathways [20, 67–71]. In this context, we selected LD-independent genome-wide significant SNPs associated with cortical phenotypes as IVs. Due to insufficient IV counts for cortical phenotype in some regions, we relaxed the threshold to 5E-06 for MR analysis. These SNPs were identified in GWAS data of cognitive performance, and their SNP-level effects were harmonized to match the effects of the alleles. The inverse variance weighted (IVW) method served as the primary approach for estimating causal effects. Additionally, we conducted MR-Egger as a sensitivity analysis [68, 72]. Significance for causal relationships was defined as $P < 0.05/180 = 0.000278$ after multiple testing.

Conjunctional false discovery rate (conjFDR) statistical framework

The conditional Q-Q plot was based on the traditional Q-Q plot, which examined the fit of the data by comparing the quantiles of observed data with the quantiles of the theoretical distribution [23, 24, 73, 74]. If the residuals of the model conform to the distribution, the points in the plot should follow the 45-degree diagonal line. Here, conditional Q-Q plots were generated by comparing the log10 (p) values of all SNP loci for cognitive performance (main trait) and log10 (p) values of SNP loci for cortical phenotypes (conditional trait) at various thresholds [23, 24].

Subsequently, we applied the conjFDR statistical framework to identify shared genetic loci between cortical phenotypes and cognitive performance. conjFDR was employed to control the error rate of simultaneously rejecting multiple null hypotheses in multiple hypothesis testing [23, 24, 75–77]. We excluded SNPs from genomic regions with complex linkage disequilibrium structures: the major histocompatibility complex (MHC) region on chromosome 6 (chr6: 25–35 Mb) and the 8p23.1 inversion region on chromosome 8 (chr8: 7–13 Mb). These regions were excluded because their extended and complex LD patterns can lead to inflated conjFDR statistics and spurious pleiotropy signals.

Definition of lead-SNPs

Using the pleioFDR package and FUMA (Functional Mapping and Annotation of Genome-Wide Association Studies), we identified independent lead-SNPs ($r^2 < 0.1$, LD blocks < 250 kb) [76, 78, 79]. By comparing the Z-scores of these lead-SNPs, we further assessed the direction of effect for shared genetic loci in each cortical structure-cognitive performance phenotype pair.

$$Z_i = \beta_i / se_i$$

Where i represents the shared loci, β_i represents the effect coefficient of i, se_i is the standard error of i. conjFDR < $0.05/180 = 0.000278$ was considered significant for shared genetic loci. Further details of the methods could be found in **Supplementary Methods** and previous studies [23, 24, 76].

Sparse canonical correlation analysis (sCCA)

Previous research defined three hierarchical structures of the S-A cortical axis, encompassing anatomical hierarchy, functional hierarchy, and evolutionary hierarchy [33–36, 45, 80–86]. Here, we employed sCCA to investigate whether the cortical genetic patterns determining cognitive performance aligned with the S-A cortical axis using mixOmics [87, 88]. sCCA achieved this by maximizing the canonical correlation between the linear combinations of two sets of variables, thereby revealing potential associations between them [89–93]. The cortical genetic patterns determining cognitive performance were defined by the number of shared genetic loci between regional cortical phenotypes and cognitive performance using conjFDR. Canonical loadings indicated the contribution and direction of the multivariate association between the cortical structure-cognitive performance genetic overlap and specific cortical hierarchy. Based on the approach outlined by Modabbernia et al., we selected the optimal sparse standard combination of parameters corresponding to the model values that maximize the sCCA correlation values [94]. Subsequently, we computed the optimal sCCA model and determined its significance based on precise p-values obtained from 1000 random permutations [94]. The p-value was defined as the number of permutations resulting in correlations equal to or higher than those observed in the original data, divided by the total number of permutations [94].

Functional annotation

To elucidate the potential functional significance of SNPs shared between cortical phenotypes and cognitive performance, we conducted RegulomeDB scoring and assessed the 15-core chromatin state [38, 78, 95, 96]. RegulomeDB scoring involved evaluating the interaction between SNPs and gene regulatory elements, such as promoters and enhancers, to assess the impact of SNPs on gene regulation [78, 97, 98]. A score of 1 indicated evidence that the SNP might influence gene expression or regulation, and/or was located within a regulatory element [78, 97]. Lower scores indicated weaker evidence. Chromatin states represented the accessibility of genomic regions (every 200 bp) with 15 categorized states [78]. States typically ≤ 7 were considered open in specific tissue/cell types. To investigate the regulated impact of these functionally significant SNPs, we performed cis-expression quantitative trait loci (eQTL) mapping in 10 brain tissues from the Braineac database and 13 brain tissues from the Genotype-Tissue Expression (GTEx) project, examining their influence on gene expression [99, 100]. Finally, we enriched shared genes between cortical phenotypes and cognitive performance in Gene Ontology (GO) and Kyoto Encyclopedia of Genes and Genomes (KEGG), aiming to infer potential biological mechanisms underlying the genetic overlap between cortical phenotypes and cognitive performance [101].

DATA AVAILABILITY

Summary GWAS statistics for cortical phenotypes was obtained from Warrier et al. [19]: https://portal.ide-cam.org.uk/overview/483. GWAS for cognitive performance (SSGAC): https://www.thessgac.org/data. GTEx: http://gtexportal.org.

CODE AVAILABILITY

LDSC: https://github.com/bulik/ldsc, TwoSampleMR: https://github.com/MRCIEU/TwoSampleMR, conjFDR: https://github.com/precimed/pleiofdr, FUMA: https://fuma.ctglab.nl/, FreeSurfer 7.3.2: https://surfer.nmr.mgh.harvard.edu/.

REFERENCES

1. Grasby KL, Jahanshad N, Painter JN, Colodro-Conde L, Bralten J, Hibar DP, et al. The genetic architecture of the human cerebral cortex. Science. 2020;367:eaay6690.
2. Vuoksimaa E, Panizzon MS, Chen CH, Fiecas M, Eyler LT, Fennema-Notestine C, et al. Is bigger always better? The importance of cortical configuration with respect to cognitive ability. Neuroimage. 2016;129:356–66.
3. Makowski C, Wang H, Srinivasan A, Qi AN, Qiu YQ, van der Mee D, et al. Larger cerebral cortex is genetically correlated with greater frontal area and dorsal thickness. Proc Natl Acad Sci USA. 2023;120:e2214834120.
4. Van Essen DC, Donahue CJ, Glasser MF. Development and evolution of cerebral and cerebellar cortex. Brain Behav Evol. 2018;91:158–69.
5. Girault JB, Cornea E, Goldman BD, Jha SC, Murphy VA, Li G, et al. Cortical structure and cognition in infants and toddlers. Cereb Cortex. 2020;30:786–800.
6. Oschwald J, Guye S, Liem F, Rast P, Willis S, Röcke C, et al. Brain structure and cognitive ability in healthy aging: a review on longitudinal correlated change. Rev Neurosci. 2020;31:1–57.
7. Karama S, Ad-Dab'bagh Y, Haier RJ, Deary IJ, Lyttelton OC, Lepage C, et al. Positive association between cognitive ability and cortical thickness in a representative US sample of healthy 6 to 18 year-olds. Intelligence. 2009;37:145–55.
8. Vuoksimaa E, Panizzon MS, Chen CH, Fiecas M, Eyler LT, Fennema-Notestine C, et al. The genetic association between neocortical volume and general cognitive ability is driven by global surface area rather than thickness. Cereb Cortex. 2015;25:2127–37.
9. Karama S, Colom R, Johnson W, Deary IJ, Haier R, Waber DP, et al. Cortical thickness correlates of specific cognitive performance accounted for by the general factor of intelligence in healthy children aged 6–18. Neuroimage. 2011;55:1443–53.
10. Fleischman DA, Leurgans S, Arfanakis K, Arvanitakis Z, Barnes LL, Boyle PA, et al. Gray-matter macrostructure in cognitively healthy older persons: associations with age and cognition. Brain Structure Funct. 2014;219:2029–49.
11. Ge T, Chen CY, Doyle AE, Vettermann R, Tuominen LJ, Holt DJ, et al. The shared genetic basis of educational attainment and cerebral cortical morphology. Cereb Cortex. 2019;29:3471–81.

12. Jansen PR, Nagel M, Watanabe K, Wei Y, Savage JE, de Leeuw CA, et al. Genome-wide meta-analysis of brain volume identifies genomic loci and genes shared with intelligence. Nat Commun. 2020;11:5606.
13. Lett TA, Vogel BO, Ripke S, Wackerhagen C, Erk S, Awasthi S, et al. Cortical surfaces mediate the relationship between polygenic scores for intelligence and general intelligence. Cereb Cortex. 2020;30:2707–18.
14. Schlaug G. Musicians and music making as a model for the study of brain plasticity. Prog Brain Res. 2015;217:37–55.
15. Worschech F, Altenmuller E, Junemann K, Sinke C, Kruger THC, Scholz DS, et al. Evidence of cortical thickness increases in bilateral auditory brain structures following piano learning in older adults. Ann N Y Acad Sci. 2022;1513:21–30.
16. Hervais-Adelman A, Moser-Mercer B, Murray MM, Golestani N. Cortical thickness increases after simultaneous interpretation training. Neuropsychologia. 2017;98:212–9.
17. Kuhl U, Friederici AD, consortium, Skeide L. MA. Early cortical surface plasticity relates to basic mathematical learning. Neuroimage. 2020;204:116235.
18. Engvig A, Fjell AM, Westlye LT, Moberget T, Sundseth O, Larsen VA, et al. Effects of memory training on cortical thickness in the elderly. Neuroimage. 2010;52:1667–76.
19. Warrier V, Stauffer EM, Huang QQ, Wigdor EM, Slob EAW, Seidlitz J, et al. Genetic insights into human cortical organization and development through genome-wide analyses of 2347 neuroimaging phenotypes. Nat Genet. 2023;55:1483–93.
20. Smith GD, Ebrahim S. Mendelian randomization': can genetic epidemiology contribute to understanding environmental determinants of disease?. Int J Epidemiol. 2003;32:1–22.
21. Davey Smith G, Hemani G. Mendelian randomization: genetic anchors for causal inference in epidemiological studies. Hum Mol Genet. 2014;23:R89–98.
22. Lee JJ, Wedow R, Okbay A, Kong E, Maghzian O, Zacher M, et al. Gene discovery and polygenic prediction from a genome-wide association study of educational attainment in 1.1 million individuals. Nat Genet. 2018;50:1112–21.
23. Andreassen OA, Djurovic S, Thompson WK, Schork AJ, Kendler KS, O'Donovan MC, et al. Improved detection of common variants associated with schizophrenia by leveraging pleiotropy with cardiovascular-disease risk factors. Am J Hum Genet. 2013;92:197–209.
24. Andreassen OA, Thompson WK, Schork AJ, Ripke S, Mattingsdal M, Kelsoe JR, et al. Improved detection of common variants associated with schizophrenia and bipolar disorder using pleiotropy-informed conditional false discovery rate. PLoS Genet. 2013;9:e1003455.
25. Glasser MF, Coalson TS, Robinson EC, Hacker CD, Harwell J, Yacoub E, et al. A multi-modal parcellation of human cerebral cortex. Nature. 2016;536:171–8.
26. van Ermingen-Marbach M, Grande M, Pape-Neumann J, Sass K, Heim S. Distinct neural signatures of cognitive subtypes of dyslexia with and without phonological deficits. Neuroimage Clin. 2013;2:477–90.
27. Caspers S, Eickhoff SB, Geyer S, Scheperjans F, Mohlberg H, Zilles K, et al. The human inferior parietal lobule in stereotaxic space. Brain Struct Funct. 2008;212:481–95.
28. Jacobs HIL, Augustinack JC, Schultz AP, Hanseeuw BJ, Locascio J, Amariglio RE, et al. The presubiculum links incipient amyloid and tau pathology to memory function in older persons. Neurology. 2020;94:e1916–e1928.
29. Babiloni C, Ferretti A, Del Gratta C, Carducci F, Vecchio F, Romani GL, et al. Human cortical responses during one-bit delayed-response tasks: an fMRI study. Brain Res Bull. 2005;65:383–90.
30. Goel V, Grafman J, Sadato N, Hallett M. Modeling other minds. Neuroreport. 1995;6:1741–6.
31. Knauff M, Mulack T, Kassubek J, Salih HR, Greenlee MW. Spatial imagery in deductive reasoning: a functional MRI study. Brain Res Cogn Brain Res. 2002;13:203–12.
32. Goel V, Gold B, Kapur S, Houle S. The seats of reason? an imaging study of deductive and inductive reasoning. Neuroreport. 1997;8:1305–10.
33. Sydnor VJ, Larsen B, Bassett DS, Alexander-Bloch A, Fair DA, Liston C, et al. Neurodevelopment of the association cortices: patterns, mechanisms, and implications for psychopathology. Neuron. 2021;109:2820–46.
34. Burt JB, Demirtas M, Eckner WJ, Navejar NM, Ji JL, Martin WJ, et al. Hierarchy of transcriptomic specialization across human cortex captured by structural neuroimaging topography. Nat Neurosci. 2018;21:1251–9.
35. Margulies DS, Ghosh SS, Goulas A, Falkiewicz M, Huntenburg JM, Langs G, et al. Situating the default-mode network along a principal gradient of macroscale cortical organization. Proc Natl Acad Sci USA. 2016;113:12574–9.
36. Xu T, Nenning KH, Schwartz E, Hong SJ, Vogelstein JT, Goulas A, et al. Cross-species functional alignment reveals evolutionary hierarchy within the connectome. Neuroimage. 2020;223:117346.
37. Sha Z, Warrier V, Bethlehem RAI, Schultz LM, Merikangas A, Sun KY et al. The overlapping genetic architecture of psychiatric disorders and cortical brain structure. bioRxiv [Preprint]. 2023. Available from: https://www.biorxiv.org/content/10.1101/2023.10.05.561040v1.full.
38. Boyle AP, Hong EL, Hariharan M, Cheng Y, Schaub MA, Kasowski M, et al. Annotation of functional variation in personal genomes using RegulomeDB. Genome Res. 2012;22:1790–7.
39. Goulding DR, Nikolova VD, Mishra L, Zhuo L, Kimata K, McBride SJ, et al. Inter-alpha-inhibitor deficiency in the mouse is associated with alterations in anxiety-like behavior, exploration and social approach. Genes Brain Behav. 2019;18:e12505.
40. Mikellidou K, Kurzawski JW, Frijia F, Montanaro D, Greco V, Burr DC, et al. Area prostriata in the human brain. Curr Biol. 2017;27:3056–3060.e3.
41. Zhao Q, Voon V, Zhang L, Shen C, Zhang J, Feng J. The ABCD study: brain heterogeneity in intelligence during a neurodevelopmental transition stage. Cereb Cortex. 2022;32:3098–109.
42. Shaw P, Greenstein D, Lerch J, Clasen L, Lenroot R, Gogtay N, et al. Intellectual ability and cortical development in children and adolescents. Nature. 2006;440:676–9.
43. Uomini N, Fairlie J, Gray RD, Griesser M. Extended parenting and the evolution of cognition. Philos Trans R Soc Lond B Biol Sci. 2020;375:20190495.
44. Giandomenico SL, Lancaster MA. Probing human brain evolution and development in organoids. Curr Opin Cell Biol. 2017;44:36–43.
45. Mesulam MM. From sensation to cognition. Brain. 1998;121:1013–52.
46. Mesulam M. Representation, inference, and transcendent encoding in neurocognitive networks of the human brain. Ann Neurol. 2008;64:367–78.
47. Luo Q, Chen Q, Wang WJ, Desrivières S, Quinlan EB, Jia TY, et al. Association of a schizophrenia-risk nonsynonymous variant with putamen volume in adolescents a voxelwise and genome-wide association study. Jama Psychiatry. 2019;76:435–45.
48. Carrera N, Arrojo M, Sanjuán J, Ramós-Ríos R, Paz E, Suárez-Rama JJ, et al. Association study of nonsynonymous single nucleotide polymorphisms in schizophrenia. Biol Psychiatry. 2012;71:169–77.
49. Scelsi MA, Khan RR, Lorenzi M, Christopher L, Greicius MD, Schott JM, et al. Genetic study of multimodal imaging Alzheimer's disease progression score implicates novel loci. Brain. 2018;141:2167–80.
50. Shin J, Ma SJ, Hofer E, Patel Y, Vosberg DE, Tilley S, et al. Global and regional development of the human cerebral cortex: molecular architecture and occupational aptitudes. Cereb Cortex. 2020;30:4121–39.
51. Shih CH, Chen CJ, Chen LY. New function of the adaptor protein SH2B1 in brain-derived neurotrophic factor-induced neurite outgrowth. PLoS One. 2013;8:e79619.
52. Hwang G, Wen J, Sotardi S, Brodkin ES, Chand GB, Dwyer DB, et al. Assessment of neuroanatomical endophenotypes of autism spectrum disorder and association with characteristics of individuals with schizophrenia and the general population. JAMA Psychiatry. 2023;80:498–507.
53. Shaw P, Kabani NJ, Lerch JP, Eckstrand K, Lenroot R, Gogtay N, et al. Neurodevelopmental trajectories of the human cerebral cortex. J Neurosci. 2008;28:3586–94.
54. Remer J, Croteau-Chonka E, Dean DC, D'Arpino S, Dirks H, Whiley D, et al. Quantifying cortical development in typically developing toddlers and young children, 1-6 years of age. Neuroimage. 2017;153:246–61.
55. Gilmore JH, Knickmeyer RC, Gao W. Imaging structural and functional brain development in early childhood. Nat Rev Neurosci. 2018;19:123–37.
56. Nelson CA, Zeanah CH, Fox NA, Marshall PJ, Smyke AT, Guthrie D. Cognitive recovery in socially deprived young children: the bucharest early intervention project. Science. 2007;318:1937–40.
57. Elliott LT, Sharp K, Alfaro-Almagro F, Shi SN, Miller KL, Douaud G, et al. Genome-wide association studies of brain imaging phenotypes in UK Biobank. Nature. 2018;562:210–6.
58. Smith SM, Douaud G, Chen W, Hanayik T, Alfaro-Almagro F, Sharp K, et al. An expanded set of genome-wide association studies of brain imaging phenotypes in UK Biobank. Nat Neurosci. 2021;24:737–45.
59. Barch DM, Albaugh MD, Avenevoli S, Chang L, Clark DB, Glantz MD, et al. Demographic, physical and mental health assessments in the adolescent brain and cognitive development study: rationale and description. Developmental Cognit Neurosci. 2018;32:55–66.
60. Glasser MF, Smith SM, Marcus DS, Andersson JLR, Auerbach EJ, Behrens TEJ, et al. The Human Connectome Project's neuroimaging approach. Nat Neurosci. 2016;19:1175–87.
61. Desikan RS, Segonne F, Fischl B, Quinn BT, Dickerson BC, Blacker D, et al. An automated labeling system for subdividing the human cerebral cortex on MRI scans into gyral based regions of interest. Neuroimage. 2006;31:968–80.
62. Schaer M, Cuadra MB, Schmansky N, Fischl B, Thiran JP, Eliez S. How to measure cortical folding from MR images: a step-by-step tutorial to compute local gyrification index. J Vis Exp. 2012;2:e3417.
63. Huang CC, Rolls ET, Feng JF, Lin CP. An extended Human Connectome Project multimodal parcellation atlas of the human cortex and subcortical areas. Brain Structure Funct. 2022;227:763–78.

64. Trampush JW, Lencz T, Knowles E, Davies G, Guha S, Pe'er I, et al. Independent evidence for an association between general cognitive ability and a genetic locus for educational attainment. Am J Med Genet Part B-Neuropsychiatric Genet. 2015;168:363–73.
65. Bulik-Sullivan B, Finucane HK, Anttila V, Gusev A, Day FR, Loh PR, et al. An atlas of genetic correlations across human diseases and traits. Nat Genet. 2015;47:1236–41.
66. Bulik-Sullivan BK, Loh PR, Finucane HK, Ripke S, Yang J, Schizophrenia Working Group of the Psychiatric Genomics C, et al. LD Score regression distinguishes confounding from polygenicity in genome-wide association studies. Nat Genet. 2015;47:291–5.
67. Burgess S, Thompson SG. Collaboration CCG. Avoiding bias from weak instruments in Mendelian randomization studies. Int J Epidemiol. 2011;40:755–64.
68. Hemani G, Zheng J, Elsworth B, Wade KH, Haberland V, Baird D, et al. The MR-Base platform supports systematic causal inference across the human phenome. Elife. 2018;7:e34408.
69. Wang T, Geng J, Zeng X, Han R, Huh YE, Peng J. Exploring causal effects of sarcopenia on risk and progression of Parkinson disease by Mendelian randomization. NPJ Parkinsons Dis. 2024;10:164.
70. Qiu S, Liu J, Guo J, Zhang Z, Guo Y, Hu Y. COVID-19 infection and longevity: an observational and mendelian randomization study. J Transl Med. 2025;23:283.
71. Qiu S, Zheng K, Hu Y, Liu G. Genetic correlation, causal relationship, and shared loci between vitamin D and COVID-19: a genome-wide cross-trait analysis. J Med Virol. 2023;95:e28780.
72. Bowden J, Davey Smith G, Burgess S. Mendelian randomization with invalid instruments: effect estimation and bias detection through Egger regression. Int J Epidemiol. 2015;44:512–25.
73. Burton PR, Clayton DG, Cardon LR, Craddock N, Deloukas P, Duncanson A, et al. Genome-wide association study of 14,000 cases of seven common diseases and 3000 shared controls. Nature. 2007;447:661–78.
74. Galwey NW. A Q-Q plot aids interpretation of the false discovery rate. Biometrical J. 2023;65:e2100309.
75. Benjamini Y, Hochberg Y. Controlling the false discovery rate - a practical and powerful approach to multiple testing. J R Stat Soc Ser B-Statistical Methodol. 1995;57:289–300.
76. Smeland OB, Frei O, Shadrin A, O'Connell K, Fan CC, Bahrami S, et al. Discovery of shared genomic loci using the conditional false discovery rate approach. Hum Genet. 2020;139:85–94.
77. Shadrin AA, Smeland OB, Zayats T, Schork AJ, Frei O, Bettella F, et al. Novel loci associated with attention-deficit/hyperactivity disorder are revealed by leveraging polygenic overlap with educational attainment. J Am Acad Child Adolesc Psychiatry. 2018;57:86–95.
78. Watanabe K, Taskesen E, van Bochoven A, Posthuma D. Functional mapping and annotation of genetic associations with FUMA. Nat Commun. 2017;8:1826.
79. Genomes Project C, Auton A, Brooks LD, Durbin RM, Garrison EP, Kang HM, et al. A global reference for human genetic variation. Nature. 2015;526:68–74.
80. Garcia-Cabezas MA, Zikopoulos B, Barbas H. The Structural Model: a theory linking connections, plasticity, pathology, development and evolution of the cerebral cortex. Brain Struct Funct. 2019;224:985–1008.
81. Hilgetag CC, Goulas A. Hierarchy' in the organization of brain networks. Philos Trans R Soc Lond B Biol Sci. 2020;375:20190319.
82. Yarkoni T, Poldrack RA, Nichols TE, Van Essen DC, Wager TD. Large-scale automated synthesis of human functional neuroimaging data. Nat Methods. 2011;8:665–70.
83. Buckner RL, Krienen FM. The evolution of distributed association networks in the human brain. Trends Cogn Sci. 2013;17:648–65.
84. Krubitzer L. The magnificent compromise: cortical field evolution in mammals. Neuron. 2007;56:201–8.
85. Donahue CJ, Glasser MF, Preuss TM, Rilling JK, Van Essen DC. Quantitative assessment of prefrontal cortex in humans relative to nonhuman primates. Proc Natl Acad Sci USA. 2018;115:E5183–E5192.
86. Wei Y, de Lange SC, Scholtens LH, Watanabe K, Ardesch DJ, Jansen PR, et al. Genetic mapping and evolutionary analysis of human-expanded cognitive networks. Nat Commun. 2019;10:4839.
87. Rohart F, Gautier B, Singh A, Le Cao KA. mixOmics: an R package for 'omics feature selection and multiple data integration. PLoS Comput Biol. 2017;13:e1005752.
88. Welham Z, Dejean S, Le Cao KA. Multivariate analysis with the R package mixOmics. Methods Mol Biol. 2023;2426:333–59.
89. Witten DM, Tibshirani R, Hastie T. A penalized matrix decomposition, with applications to sparse principal components and canonical correlation analysis. Biostatistics. 2009;10:515–34.
90. Mihalik A, Chapman J, Adams RA, Winter NR, Ferreira FS, Shawe-Taylor J, et al. Canonical correlation analysis and partial least squares for identifying brain-behavior associations: a tutorial and a comparative study. Biol Psychiatry Cogn Neurosci Neuroimaging. 2022;7:1055–67.
91. Grellmann C, Bitzer S, Neumann J, Westlye LT, Andreassen OA, Villringer A, et al. Comparison of variants of canonical correlation analysis and partial least squares for combined analysis of MRI and genetic data. Neuroimage. 2015;107:289–310.
92. Wang T, Shu H, Hu J, Wang Y, Chen J, Peng J, et al. Accurately deciphering spatial domains for spatially resolved transcriptomics with stCluster. Brief Bioinform. 2024;25:bbae329.
93. Zhang X, Chen J, Wang Y, Wang X, Hu J, Peng J, et al. cfMethylPre: deep transfer learning enhances cancer detection based on circulating cell-free DNA methylation profiling. Brief Bioinform. 2025;26:bbaf303.
94. Modabbernia A, Reichenberg A, Ing A, Moser DA, Doucet GE, Artiges E, et al. Linked patterns of biological and environmental covariation with brain structure in adolescence: a population-based longitudinal study. Mol Psychiatry. 2021;26:4905–18.
95. Kircher M, Witten DM, Jain P, O'Roak BJ, Cooper GM, Shendure J. A general framework for estimating the relative pathogenicity of human genetic variants. Nat Genet. 2014;46:310–5.
96. Wang T, Luo Z. Large language models transform biological research: from architecture to utilization. Sci China Inf Sci. 2025;68:170101.
97. Dong SC, Zhao NX, Spragins E, Kagda MS, Li MJ, Assis P, et al. Annotating and prioritizing human non-coding variants with RegulomeDB v.2. Nat Genet. 2023;55:724–6.
98. Cao C, Wang C, Dai Q, Zou Q, Wang T. CRBPSA: CircRNA-RBP interaction sites identification using sequence structural attention model. BMC Biol. 2024;22:260.
99. Lonsdale J, Thomas J, Salvatore M, Phillips R, Lo E, Shad S, et al. The genotype-tissue expression (GTEx) project. Nat Genet. 2013;45:580–5.
100. Ardlie KG, DeLuca DS, Segrè AV, Sullivan TJ, Young TR, Gelfand ET, et al. The Genotype-Tissue Expression (GTEx) pilot analysis: multitissue gene regulation in humans. Science. 2015;348:648–60.
101. Yu G, Wang LG, Han Y, He QY. clusterProfiler: an R package for comparing biological themes among gene clusters. OMICS. 2012;16:284–7.

ACKNOWLEDGEMENTS

This work was supported by the National Natural Science Foundation of China (No. 62371161, 62331012), Key Research and Development Program of Heilongjiang Province (No. 2022ZX02C20), Research and Innovation Fund of The First Affiliated Hospital of Harbin Medical University (No. 2021M13), and 0–1 Original Exploration Category: Fundamental Research Funds for the Central Universities Project (No. 2022FRFK030025). The funders did not participate in analysis or writing of this report. We thank the participants in all the GWASs used in this manuscript and Warrier et al. and other investigators who made these GWAS data publicly available.

AUTHOR CONTRIBUTIONS

Y.H., J.L., and Y.W. conceived, designed, and supervised the project. S.Q. implemented statistical analyses and drafted the manuscript. Y.H., J.G., and Z.Z. accessed and verified the underlying data reported in the manuscript. J.L., Y.H., J.G., Z.Z., H.L., and H.Y. contributed to suggestions on analysis strategy and findings interpretation. All authors critically revised the content and contributed to editing the paper.

COMPETING INTERESTS

The authors declare no competing interests.

ETHICS APPROVAL AND CONSENT TO PARTICIPATE

All methods were performed in accordance with the relevant guidelines and regulations. This research consisted of secondary data analysis using existing published datasets and public resources. Each contributing study involving humans was approved by the relevant ethics committees and informed consent was obtained from all participants for the primary studies. UK Biobank has approval from the North West Multi-centre Research Ethics Committee (MREC) as a Research Tissue Bank (RTB) approval. This approval means that researchers do not require separate ethical

clearance and can operate under the RTB approval. No live vertebrates were involved in this research.

ADDITIONAL INFORMATION

Supplementary information The online version contains supplementary material available at https://doi.org/10.1038/s41398-025-03803-8.

Correspondence and requests for materials should be addressed to Yang Hu, Jingjing Liu or Yadong Wang.